Paper ID APEN-MIT-2020_312
Applied Energy Symposium: MIT A+B
August 12-14, 2020 • Cambridge, USA

A Novel High Energy Density Sorption-based Thermal Battery for Low-grade Thermal Energy Storage

Lingshi Wang
Energy and Transportation Science Division
Oak Ridge National Laboratory
Oak Ridge, TN, USA
wangl2@ornl.gov

Xiaobing Liu
Energy and Transportation Science Division
Oak Ridge National Laboratory
Oak Ridge, TN, USA
liux2@ornl.gov

Kyle R. Gluesenkamp
Energy and Transportation Science Division
Oak Ridge National Laboratory
Oak Ridge, TN, USA
gluesenkampk@ornl.gov

Zhiyao Yang
Energy and Transportation Science Division
Oak Ridge National Laboratory
Oak Ridge, TN, USA
yangz1@ornl.gov

Abstract— Thermal energy storage (TES) can alleviate peak demand on the electricity grid by offsetting building thermal loads, increasing the grid's reliability and resilience. However, low energy density and poor energy performance of existing TES technologies limit their applications. Sorption-based thermal battery (STB) system is thus developed using three-phase sorption technology to harvest low-temperature heat, store it with a much higher energy density than common TES systems and dehumidify air or provide space cooling in buildings. Although STB has been experimentally proved to be feasible, influencing factors on its performance are still unknown by far. Therefore, this paper conducted a parametric analysis on crystallization and crystal dissolution performance of a developed STB test rig. The crystallization results showed that the energy density of the STB increased with reducing the solution flow rate and the cooling water temperature. The dissolution results showed that a higher discharge rate of the STB can be achieved with increasing the flow rate and temperature of inlet diluted solution. The work in this study is helpful to the optimal design and operation of the STB system.

Keywords—sorption-based thermal battery, crystallization, thermal energy storage, energy density, experimental investigation

I. INTRODUCTION

Buildings consume a large amount of electricity energy, of which 40–70% meets its thermal demands, such as space cooling, space heating, and water heating. It is a big challenge for the electricity grid to meet the peak demand of buildings. Meanwhile, the thermal loads in buildings can be also fulfilled by renewable or low-temperature energy, such as solar energy, industrial waste heat, and low-temperature (<150°C) geothermal energy [1]. However, there exists both temporal and distance gaps between the low-grade heat resource and the thermal demand. For example, the peak cooling demand in residential buildings usually occurs in the evening while the peak solar energy occurs in the afternoon. The existing low-temperature geothermal resources are highly localized and the energy need to be transported over long distances for end use [2].

One solution to alleviate peak demand on the electricity grid and expand the utilization of the low-grade energy is using thermal energy storage (TES) technologies to offset building thermal loads. Conventional thermal energy storage technologies use either sensible heat of chilled or hot water [3] or the latent heat of a phase change material (PCM) [4] or ice [5]. The energy storage density (ESD) of a TES technology using sensible heat depends on the temperature difference between the energy resource and the thermal demand. For storing heat in water with a temperature of 40–90°C, the ESD is low (209 kJ/kg), and heavy insulation is needed to reduce heat loss to the environment. TES using latent heat of PCM offers higher ESD, but the ESD is usually lower than 350 kJ/kg and it also needs to be insulated to reduce heat loss during storage and transportation.

Compared to above TES technologies, absorption thermal energy storage offers higher energy storage density by using vaporization and condensation heat of medium such as water or ammonia without heat loss problems, thus it attracts more and more attentions in recent years [6]. Absorption thermal energy storage is compatible with heating, cooling or simultaneous cooling and heating application with only heating energy input [7]. A prototype of a lithium bromide/water ($LiBr/H_2O$) absorption TES system was built [8], sodium hydroxide (NaOH) solution was also used in the European Union (EU) COMTES project [9,10] for solar heat storage. A dynamic model for a long-term closed solar absorption TES system for building heating was also developed [11]. To improve the energy storage density of the absorption TES system, a closed three-phase absorption TES device named Thermo-Chemical Accumulator (TCA) was developed by effectively generating crystals from the energy storage solution [12].

A novel absorption TES system, sorption-based thermal battery (STB), was invented at Oak Ridge National Laboratory (ORNL) by Liu et al. [13] and Yang et al. [14]. The STB can be used as either a stationary TES device or a mobile device being transported back and forth between heat resources and thermal demands, which is charged (storing energy) and discharged (releasing energy) at different times of the day or year. The ESD of a STB is determined by the selection of the energy storage medium and thermal applications where the stored energy is used. Studies showed that storing heat by making lithium chloride (LiCl) hydrate crystals and releasing the stored latent heat for air dehumidification results in the highest ESD among all the investigated scenarios [14]. Furthermore, the LiCl solution can be generated at a relatively low temperature (75ºC), which indicates a good fit for utilizing low-temperature energy. A benchtop prototype STB and the related experimental apparatus have been established and tested at the ORNL to evaluate its performance of both charge and discharge processes. Experimental results showed that the LiCl crystals were successfully generated and were also effectively dissolved. An energy storage density of 903 kJ/kg has been achieved by the prototype for liquid desiccant dehumidification application [15].

The ESD of a STB depends on how many salt crystals can be produced in it, and the discharge rate (i.e. latent cooling capacity) of a STB is determined by how quick the salt crystals in the STB can be dissolved. However, there is still a lack of research on the characteristics of crystallization and dissolution of STB. Therefore, this study presents a parametric analysis on the performance of crystallization and dissolution of a developed STB, the investigated factors influencing the crystallization process include the solution flow rate and the cooling water temperature, and influencing the dissolution process include the flow rate and temperature of inlet diluted solution. Experimental results under different test conditions will be compared.

II. Experimental Apparatus of Sorption-Based Thermal Battery System

A benchtop prototype STB was designed and built (Figure 1). The main body of prototype STB is a cylindrical tank made of acrylic organic glass with an inner diameter of 15.2 cm, an outer diameter of 16.5 cm, and a height of 27.9 cm. A helical coil made with stainless steel was inserted in the tank's center for heat exchange between a thermal bath and the stored solution in the STB. Fine-mesh plastic filters were applied at the top and bottom of the tank to prevent salt crystals escaping from the tank. LiCl aqueous solution was adopted as the energy storage medium, it flowed in through the bottom inlet of the STB and flowed out of the top outlet of the STB.

To characterize the formation and dissolution processes of hydrate crystals in the STB, and investigate the impact factors of its crystallization and crystal dissolution performance, an experimental apparatus was developed, as show in Figure 1. The experimental apparatus comprises a prototype STB with a capacity of 5 litre (L), two identical solution tanks (each has a capacity of 10 L) with immersed helical heat exchanger, two piping systems (including identical circulation pump and control valves), and two thermal baths. The flow rate of the LiCl solution feeding into

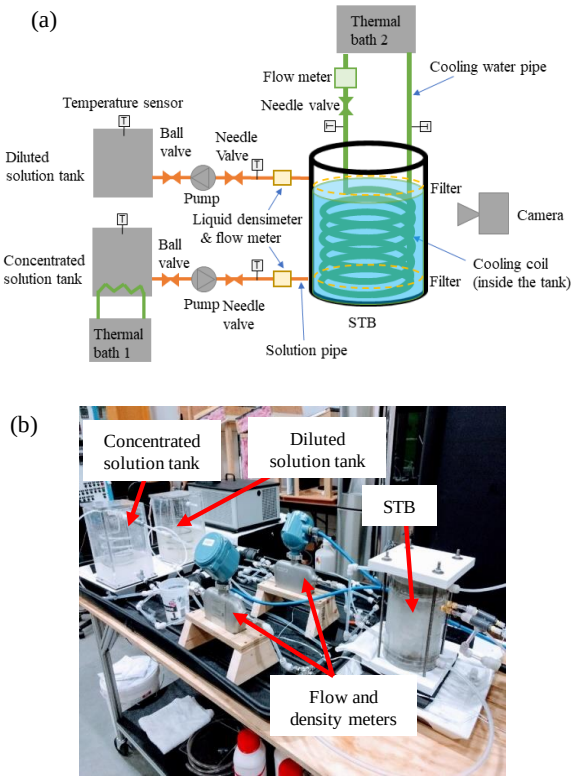

Fig. 1. (a) A schematic of the experimental apparatus of STB; (b) A photo of the experimental apparatus of STB.

the STB was adjusted by a needle valve and the concentration and temperature the LiCl solution feeding into the STB were controlled in the solution tank. One thermal bath was used to control solution temperature in the solution tank and another thermal bath was used to control cooling/heating temperature of stored solution in the STB.

The crystallization test is as follows. First, the STB was filled with hot and concentrated LiCl solution which simulated the solution generated from the regenerator. Then the concentrated solution in the STB was cooled by the cooling water from a thermal bath and crystallized on the surface of the heat exchanger in the STB. Meanwhile the hot solution in the concentrated solution tank with the same temperature and concentration was supplied to the STB and the diluted solution in the STB after crystallizing was exhausted to diluted solution tank. When the STB was saturated with salt crystals, a dissolution test can be conducted. First, the prepared warm and diluted solution was pumped from the diluted solution tank into the STB to dissolve the salt crystals. The concentrated solution after dissolving the salt crystals was pumped out from the STB into the concentration solution tank. The concentrated solution can be used for absorption cooling/heating or dehumidification.

Temperatures were measured with four-wire resistance temperature detectors except the temperatures of the solution tanks were measured with T-type thermocouples. Flow rate of cooling water was measured with an electromagnetic flowmeter. Flow rate and density of LiCl solution flowed into and out of the STB were measured with two Micro Motion Coriolis flow and density meters, respectively. The measured data were recorded with a data acquisition system.

The crystallization and dissolution processes were also visually recorded by a camera. The specifications of the measurement instruments are available in literature [15].

The performance of STB can be evaluated with two indicators: the ESD for the energy charge process and the discharge rate (Q_d) for the energy discharge process.

The ESD of a STB is determined by the selected energy storage medium and its thermal application. ESD is calculated with Eq. (1):

$$ESD = \frac{M_w\ q_v}{M_{s,d}} \tag{1}$$

where $M_{s,d}$ is the mass of diluted halide salt solution after the discharge process (kg), M_w is the mass of water released from the diluted solution after the charging process (kg), and q_v is the latent heat of vaporization per unit mass of water (kJ/kg).

The crystal fraction (i.e., the ratio of crystal mass to the total mass in the STB) (F_c) in the STB after the crystallization process is calculated by Eq. (2):

$$F_c = \frac{M_c}{M_s} \tag{2}$$

where M_c is total mass of salt crystals (kg), M_s is the mass of solution before the discharge process (kg).

The STB's discharge rate (Q_d) is used to evaluate the dissolution performance. When the discharge system uses liquid desiccant solution dissolved from the STB, Q_d is actually the latent cooling capacity for dehumidifying air and can be calculated by Eq. (3):

$$Q_d = (\frac{m_{out}\,X_{out}}{X_d} - m_{out})q_v \tag{3}$$

where m_{out}, X_{out}, and X_d represent the mass flow rate (kg/m^3), concentration (-) of outlet solution from STB and the diluted solution concentration (-) after the discharge process, respectively.

The detailed calculations for the values of ESD, F_c and Q_d can be found in literature [15].

III. Parametric Analysis on Crystallization and Crystal Dissolution Performance

A parametric study was performed to investigate the impacts of several operating variables on the crystallization and dissolution performance of the STB. Energy storage density and crystal fraction in the STB during the crystallization process were compared under different solution flow rates and cooling water temperatures, respectively. The discharge rate of the dissolution process was also compared under different solution flow rates and solution temperatures, respectively.

A. *Crystallization performance*

The crystallization tests were conducted with three solution flow rates, 1.58 g/s, 2.04 g/s and 5.02 g/s, respectively, as listed in Table 1. Other test conditions were remained nearly identical during these tests. The concentration and temperature of the inlet strong solution from the concentrated solution tank to the STB were kept at 50 % and ~ 60 ºC, respectively, and the inlet cooling water temperature from the thermal bath to the STB was maintained at 20.4 °C.

The ESD and F_c resulting from these three tests are shown in Figure 2. It indicated that the ESD and F_c decreased with the increase of solution flow rate under the same cooling condition. In order to achieve a high ESD, a low solution flow rate is needed. The maximum ESD obtained from these tests was 981.8 kJ/kg at a solution flow rate of 1.58 g/s, and the maximum F_c achieved in these tests was 51.1% when the solution flow rate was at 1.58 g/s. The crystal fraction dropped to only 12.1% when the solution flow rate was increased to 5.02 g/s.

Although a lower solution flow rate can result in a higher ESD, it also increases the risk of blockage inside the piping system of the STB because the strong solution can quickly crystallize inside the piping system when the solution flow is low. Therefore, an optimal solution flow rate needs to be identified in the future study to maximize the ESD while keeping the solution flowing continuously.

The impacts of cooling water temperatures on the crystallization performance were also experimentally investigated. The three test conditions are shown in Table 2. Three investigated cooling water temperatures were 11.1 ºC, 20.4 ºC and 29.7 ºC, respectively. Other test conditions were remained identical during the three tests.

The ESD and F_c for these three tests are shown in Figure 3. As can be seen from this figure, ESD and F_c decreased with the increase of inlet cooling water temperature. When the inlet cooling temperature was increased from 11.1 ºC to 29.7 ºC, the ESD decreased from 817.4 kJ/kg to 714.1 kJ/kg, while the F_c decreased from 21.9% to 11.4%. The reason for this result is that the saturation concentration of the solution after crystallization in the STB increased at a higher cooling water temperature. Therefore, the driving force (the difference between the concentration of the strong solution and the equilibrium concentration for crystallization) for the crystallization was reduced.

TABLE 1. TEST CONDITIONS OF CRYSTALLIZATION WITH DIFFERENT SOLUTION FLOW RATES.

$m_{s,in}$ (g/s)	$X_{s,in}$ (%)	$T_{s,in}$ (ºC)	m_w (L/min)	$T_{w,in}$ (ºC)	$T_{w,out}$ (ºC)
1.58	50.1	60.6	0.90	20.4	21.8
2.04	50.3	64.0	0.90	20.4	21.8
5.02	49.6	61.1	0.89	20.4	21.8

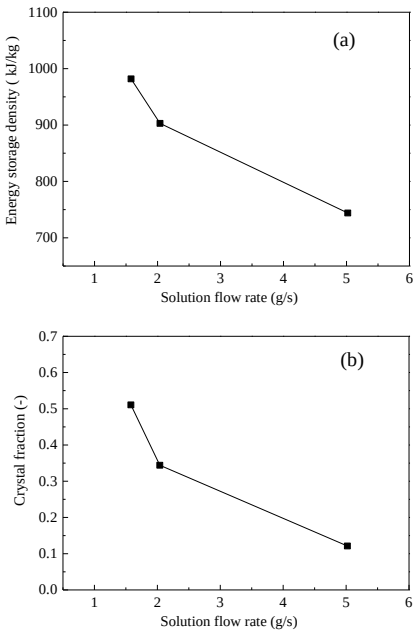

Fig. 2. Influence of solution flow rate on (a) energy storage density; (b) crystal fractions.

TABLE 2. TEST CONDITIONS OF CRYSTALLIZATION WITH DIFFERENT COOLING WATER TEMPERATURES.

$m_{s,in}$ (g/s)	$X_{s,in}$ (%)	$T_{s,in}$ (°C)	m_w (L/min)	$T_{w,in}$ (°C)	$T_{w,out}$ (°C)
5.76	49.9	62.2	0.82	11.1	13.4
5.02	49.6	61.1	0.89	20.4	21.8
5.01	50.0	65.7	0.97	29.7	30.6

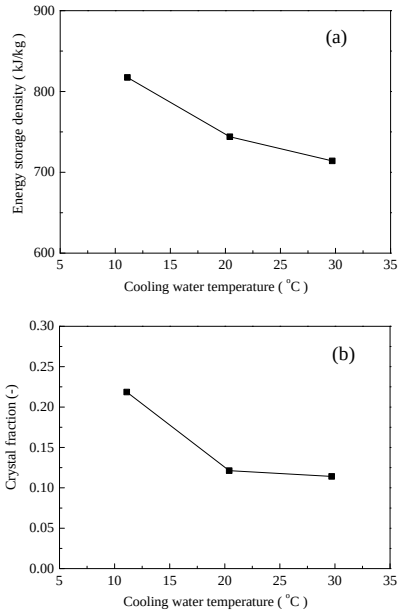

Fig. 3. Influence of cooling water temperature on (a) energy storage density; (b) crystal fraction.

TABLE 3. DISSOLUTION TEST CONDITIONS WITH DIFFERENT SOLUTION FLOW RATES.

$m_{s,in}$ (g/s)	$X_{s,in}$ (%)	$T_{s,in}$ (°C)
2.41	35.2	40.5
5.90	35.1	40.9
8.72	34.9	40.4

B. Dissolution performance

The impacts of solution flow rate were studied for the dissolution process. Table 3 shows the three test conditions with different solution flow rates, i.e. 2.41 g/s, 5.90 g/s and 8.72 g/s, respectively. Concentration and temperature of inlet solution from the diluted solution tank to the STB were remained nearly identical during the three tests.

The results of discharge performance are shown in Figure 4. These results indicated that the maximum discharge rate increased with the increase of solution flow rate, as the mixing of solution with crystals in the STB was enhanced with a higher solution flow rate. When the solution flow rate was increased from 2.41 g/s to 8.72 g/s, the maximum discharge rate increased from 0.95 kW to 1.5 kW, while the time needed for totally dissolving the crystals reduced from 28 min to 15 min. The higher of the solution flow rate, the shorter and less stable the discharge process would be. It is because that the total amount of salt crystals stored in the STB was fixed, thus a higher discharge rate at the beginning resulted in a faster decay of the discharge rate. Therefore, both the discharge rate and the needed stable duration time should be accounted for when determining the size and solution flow rate of a STB system.

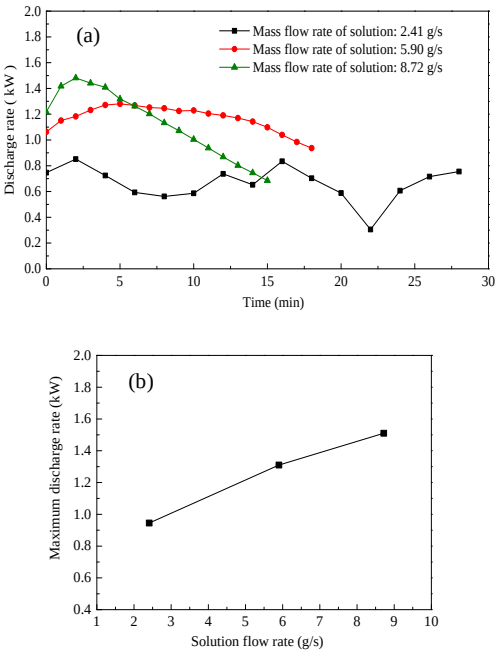

Fig. 4. Discharge performance with different solution flow rates: (a) discharge rate over time; (b) maximum discharge rate.

TABLE 4. DISSOLUTION TEST CONDITIONS WITH DIFFERENT INLET SOLUTION TEMPERATURES.

$m_{s,in}$ (g/s)	$X_{s,in}$ (%)	$T_{s,in}$ (°C)
5.90	35.1	40.9
5.52	35.1	50.0

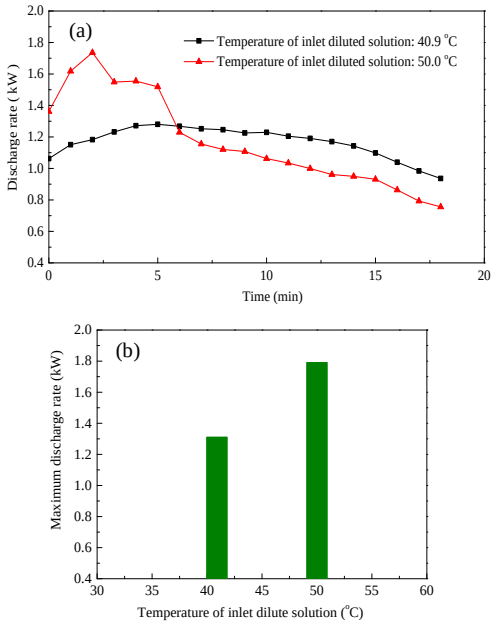

Fig. 5. Discharge performance with different inlet solution temperatures: (a) discharge rate over time; (b) maximum discharge rate

Two tests with different inlet solution temperatures from the diluted solution tank to the STB, i.e. 40.9 °C and 50.0 °C, were conducted, the test conditions are shown in Table 4. Concentration and mass flow rate of the inlet solution were kept constant during the two tests. Figure 5 indicated that the higher the inlet solution temperature, the higher the maximum discharge rate. That's because the solution has a higher saturation concentration at a higher temperature to dissolve the crystals. The maximum discharge rate reached 1.79 kW when the inlet solution temperature was 50.0 °C, but it didn't last for a long time due to the limited capacity of the STB for energy release. Since the 50.0 °C solution temperature is higher than the temperature of a diluted LiCl solution leaving a desiccant cooling system, which usually ranging from 30 to 35 °C, pre-heating is thus needed. Renewable or low-grade energy (such as the solar energy) can be used for pre-heating the solution.

IV. CONCLUSIONS

This paper presents a parametric study on crystallization and dissolution performance of a sorption-based thermal battery (STB) system which used lithium chloride (LiCl) for energy storage. The impacts of different operating variables on the crystallization and dissolution performance were experimentally investigated and compared. The results showed that the energy storage density and the crystal fraction of the STB increased with a decrease in the solution flow rate and the cooling water temperature, while the discharge rate (i.e., latent cooling capacity for dehumidifying air) increased with increasing the solution flow rate and the temperature of the diluted solution. However, the discharge process was shorter and less stable with a higher flow rate, which indicated that needed stable duration time at a required discharge rate also should be accounted for when designing a STB system. The maximum energy storage density achieved in the crystallization tests was 981.8 kJ/kg, and the maximum discharge rate achieved in the dissolution tests was up to 1.79 kW. The results demonstrated the technical feasibility of the STB system and proved that the STB can achieve a higher energy density than other thermal storage technologies. The results in this study can be used for the design guide of the STB system.

In order to further improve the performance of STB, future work is recommended to improve the design of STB's heat exchanger to increase the energy storage density and discharge rate and develop a mathematic model of the STB to simulate the performance for its optimal design and operation.

ACKNOWLEDGMENT

This research was supported by the DOE Office of Energy Efficiency and Renewable Energy, Geothermal Technologies Office. The authors would also like to acknowledge Ms. Arlene Anderson and Joshua Mengers of the Geothermal Technologies Office. This manuscript has been authored by UT-Battelle, LLC under Contract No. DE-AC05-00OR22725 with the U.S. Department of Energy. The United States Government retains and the publisher, by accepting the article for publication, acknowledges that the United States Government retains a non-exclusive, paid-up, irrevocable, world-wide license to publish or reproduce the published form of this manuscript, or allow others to do so, for United States Government purposes. The Department of Energy will provide public access to these results of federally sponsored research in accordance with the DOE Public Access Plan (http://energy.gov/downloads/doe-public-access-plan).

REFERENCES

[1] DOE. "Direct Use of Geothermal Energy." Available at http://energy.gov/eere/geothermal/direct-use-geothermal-energy, (2015).

[2] OIT Geo-Heat Center. "Geothermal Direct-Use Case Studies." (2005). Accessed May 12, 2019. https://www.oit.edu/orec/geo-heat-center/case-studies. Accessed: 5/12/2019

[3] Cui, B., et al. Life-cycle cost benefit analysis and optimal design of small scale active storage system for building demand limiting. Energy 2014;73: 787-800.

[4] Cabeza, L. F., Castell, A., Barreneche, C. D., De Gracia, A., and Fernández, A. I. Materials used as PCM in thermal energy storage in buildings: a review. Renewable and Sustainable Energy Reviews, 2011;15(3): 1675-1695.

[5] Ibrahim, N. I., et al. Experimental testing of the performance of a solar absorption cooling system assisted with ice-storage for an office space. Energy Conversion and Management 2017;148: 1399-1408.

[6] Yu, N., R.Z. Wang, L.W. Wang. Sorption thermal storage for solar energy. Progress in Energy and Combustion Science 2013; 39(5): 489-514.

[7] Rosato, A., S. Sibilio. Preliminary experimental characterization of a three-phase absorption heat pump. International Journal of Refrigeration 2013; 36: 717-729.

[8] Zhang, X., M. Li, W. Shi, B. Wang, X. Li. Experimental investigation on charging and discharging performance of absorption thermal energy storage system. Energy Conversion and Management 2014; 85(Supplement C): 425-434.

[9] Fumey, B., Weber, R., Gantenbein, P., Daguenet-Frick, X., Williamson, T., and Dorer, V. Development of a closed sorption heat storage prototype. Energy Procedia 2014; 46: 134-141.

[10] Koll, J., Helden, W.V., and Fumey, B. COMTES project. http://comtes-storage.eu/, (2015).

[11] N'Tsoukpoe, K.E., N. Le Pierrès, L. Luo. Numerical dynamic simulation and analysis of a lithium bromide/water long-term solar heat storage system. Energy 2012; 37(1): 346-358.

[12] Bales, C, S. Nordlander. 2005. TCA evaluation-lab measurements, modelling and system simulations. Borlange, Sweden: Hogskolan Dalarna, www.serc.se

[13] Liu, X., Yang, Z., Gluesenkamp, K. R., & Momen, A. M. A Technical and Economic Analysis of an Innovative Two-Step Absorption System for Utilizing Low-Temperature Geothermal Resources to Condition Commercial Buildings. ORNL/TM-2015/655, Oak Ridge National Laboratory, Oak Ridge, TN (2015).

[14] Yang, Z., et al. Transported Low Temperature Geothermal Energy for Thermal End Uses—Final Report. ORNL/TM-2016/658, Building Technologies Research and Integration Center (BTRIC), Oak Ridge National Laboratory (ORNL), Oak Ridge, TN (2016).

[15] Wang, L., X. Liu, Z. Yang, K.R. Gluesenkamp. Experimental study on a novel three-phase absorption thermal battery with high energy density applied to buildings. Energy, 2020, 208:118311.